





Article

Assessing Soil Erosion by Monitoring Hilly Lakes Silting

Yamuna Giambastiani ^{1,*}, Riccardo Giusti ¹, Lorenzo Gardin ¹, Stefano Cecchi ¹, Maurizio Iannuccilli ¹, Stefano Romanelli ², Lorenzo Bottai ², Alberto Ortolani ^{1,2} and Bernardo Gozzini ^{1,2}

¹ CNR-IBE, National Research Council, Institute of Bioeconomy, 50019 Florence, Italy; giusti@lamma.toscana.it (R.G.); gardin@lamma.toscana.it (L.G.); cecchi@lamma.toscana.it (S.C.); iannuccilli@lamma.toscana.it (M.I.); ortolani@lamma.toscana.it (A.O.); gozzini@lamma.toscana.it (B.G.)

² Environmental Modelling and Monitoring Laboratory for Sustainable Development, LaMMA Consortium, 50019 Florence, Italy; romanelli@lamma.toscana.it (S.R.); bottai@lamma.toscana.it (L.B.)

* Correspondence: giambastiani@lamma.toscana.it

Abstract: Soil erosion continues to be a threat to soil quality, impacting crop production and ecosystem services delivery. The quantitative assessment of soil erosion, both by water and by wind, is mostly carried out by modeling the phenomenon via remote sensing approaches. Several empirical and process-based physical models are used for erosion estimation worldwide, including USLE (or RUSLE), MMF, WEPP, PESERA, SWAT, etc. Furthermore, the amount of sediment produced by erosion phenomena is obtained by direct measurements carried out in experimental sites. Data collection for this purpose is very complex and expensive; in fact, we have few cases of measures distributed at the basin scale to monitor this phenomenon. In this work, we propose a methodology based on an expeditious way to monitor the volume of hilly lakes with GPS, sonar sensor and aquatic drone. The volume is obtained by means of an automatic GIS procedure based on the measurements of lake depth and surface area. Hilly lakes can be considered as sediment containers. Time-lapse measurements make it possible to estimate the silting rate of the lake. The volume of 12 hilly lakes in Tuscany was measured in 2010 and 2018, and the results in terms of silting rate were compared with the estimates of soil loss obtained by RUSLE and MMF. The analyses show that all the lakes measured are subject to silting phenomena. The sediment estimated by the measurements corresponds well to the amount of soil loss estimated with the models used. The relationships found are significant and promising for a distributed application of the methodology, which allows rapid estimation of erosion phenomena. Substantial differences in the proposed comparison (mainly found in two cases) can be justified by particular conditions found on site, which are difficult to predict from the models. The proposed approach allows for a monitoring of basin-scale erosion, which can be extended to larger domains which have hilly lakes, such as, for example, the Tuscany region, where there are more than 10,000 lakes.

Keywords: sediment monitoring; remote sensing; lakes; water capacity; sonar; aquatic drone; USLE; MMF



Citation: Giambastiani, Y.; Giusti, R.; Gardin, L.; Cecchi, S.; Iannuccilli, M.; Romanelli, S.; Bottai, L.; Ortolani, A.; Gozzini, B. Assessing Soil Erosion by Monitoring Hilly Lakes Silting. *Sustainability* **2022**, *14*, 5649. <https://doi.org/10.3390/su14095649>

Academic Editors: Blaž Repe, Mario Elia and Antonio Ganga

Received: 30 March 2022

Accepted: 3 May 2022

Published: 7 May 2022

Publisher's Note: MDPI stays neutral with regard to jurisdictional claims in published maps and institutional affiliations.



Copyright: © 2022 by the authors. Licensee MDPI, Basel, Switzerland. This article is an open access article distributed under the terms and conditions of the Creative Commons Attribution (CC BY) license (<https://creativecommons.org/licenses/by/4.0/>).

1. Introduction

1.1. Erosion: A Worldwide Threat

After almost a century of research and studies on the territory, soil erosion caused by water, wind and tillage is known to be the greatest threat to soil health, and to the ecosystem services it provides, in many regions of the world [1–3]. Its impact on global crop production has been estimated at a reduction of 0.4% per year [4]. Some authors argue that nearly a third of the world's arable land has been lost due to erosion over the past 40 years and continues to decrease at a rate greater than ten million hectares per year [5]. Erosion is a natural phenomenon which consists of the loss of the most superficial layer of the soil due to the action of precipitation or wind. With the advent of modern agriculture and, above all, with (I) the introduction of extensive mechanization, (II) the leveling of the

slopes, (III) the abandonment of traditional hydraulic-agricultural solutions and (IV) the specialization of crops, erosion has assumed worrying proportions [6–8]. Erosion is now a worldwide threat, especially in hilly areas with significant economic impacts, particularly in areas with valuable crops [9,10]. Water erosion represents one of the main threats to the correct functionality of the soil, through (I) the removal of the fertile surface soil horizon, (II) the denser subsoil incorporation in the surface layer and (III) the possible decrease in the root zone [11].

A reliable assessment of this phenomenon is therefore particularly useful as a decision-support tool for planning soil conservation interventions [12–14]. To address these issues, the Community Agricultural Policy has ensured that agriculture is in line with the EU soil protection policies. Effective management of these issues is considered essential for many strategies and priorities of the European Green Deal, as defined primarily in the (I) thematic strategy and the sustainable management of soil [15], (II) the fight against erosion, and (III) the fight against the loss of organic carbon and biodiversity in soil. The quantitative assessment of soil erosion, due to both water and wind, is generally carried out through modeling the phenomenon or with experimental tests (plots, rain simulators, etc.) carried out directly on the field [16]. In recent decades, researchers in Italy have also conducted several direct studies on the phenomenon of erosion [17–22].

1.2. Models for Erosion Estimation

The most commonly used erosion estimation model is the universal equation of soil loss (USLE) [23], and its revised version (RUSLE) [24], which estimates the annual mean long-term loss of soil due to sheet (interrill) and rill erosion. It should be noted that soil loss caused by (ephemeral) gully erosion is not predicted by RUSLE [25]. Despite its shortcomings, RUSLE is still the most widely used model on a large scale [26,27]. It can process data input for large regions and provides a basis for scenario analysis and taking actions against erosion [28]. A recent work [29] estimated erosion on a European scale using the most in-depth processing of the single factors [29–32]. USLE has been applied in comparative studies between various analysis methods, and the authors have shown that it does not lead to greater errors than process-based physical models (WEPP and PESERA), although it has some limitations due to the simple empirical nature of the model [33–35]. Soil loss is also analyzed worldwide through the revised MMF—Morgan–Morgan–Finney model [36,37], in order to evaluate the land degradation and ecological status of specific catchment areas or wider territories [38–40]. This model allows an erosion simulation to be developed in relation to the characteristics of the vegetation cover. The comparison between these empirical models shows similar results [41,42]. The Soil and Water Assessment Tool (SWAT) is a semi-empirical model used for the assessment of erosion phenomena at the basin scale [43–45]. It also allows analyses related to hydrological processes [46], land management and climate change [47,48]. Other simulations have been performed directly on reconstructions of hydrographic basins in miniature or in experimental sites [49–51].

In Tuscany in 2009, soil erosion estimates were made at a regional scale with the USLE model through the elaboration of single climatic, pedological, land use and morphometric factors at high resolution [52,53]. Direct measurements carried out over the years in experimental fields [54–56] have allowed the model to be properly constrained and tested.

1.3. Scope of Work

With this work, we propose a new approach to monitor erosion phenomena at the basin scale, based on an expeditious estimate of the hilly lakes silting rate, through remote sensing techniques. The basic assumption is that a relationship exists between the soil loss (or sediment production) from the basin with the volume loss of the reservoir. The silting rate, estimated by sonar and aquatic drone [57], is compared with the soil loss obtained from two models (RUSLE and MMF) in order to evaluate erosion through direct measurements of the sediment produced. The hilly lakes distributed throughout the territory can be considered the containers of the sediment coming from the erosion phenomena of the

slope, and therefore constitute a net of distributed monitoring. This expeditious method of estimating the reservoir capacity for the study of erosion phenomena is an innovative tool that enables the estimation of the sediment produced by a slope. The aim is to demonstrate that through the repetition over time of a simple procedure of silting estimation, it is possible to observe the evolution of the erosive phenomena and better understand the impact of anthropogenic actions or climate change on the quality of soils. In Tuscany, there are about 5000 lakes with a surface greater than 1000 square meters, which can become the mean for the distributed monitoring of erosive phenomena.

2. Materials and Methods

2.1. Lakes Analyzed and Volume Changes

The study took into consideration 12 hilly lakes in Tuscany, shown in Figure 1, of which the volume calculated in 2010 is known, thanks to a past survey by the former Agency for Development and Innovation in Agriculture (ARSIA) of Regione Toscana (RT—regional administration of Tuscany). The volume estimate was carried out by a private company (Aquaterra, Florence) using a boat, a depth sounder and GPS, thus carrying out a bathymetric survey [58]. LaMMA Consortium, applying the methodology described by Giambastiani et al. 2020 [57], measured the lakes again in 2018 thanks to a monitoring project. We assume that the two methodologies are comparable, as the same types of tools and procedures are used. Furthermore, the measurements were carried out for both years in early spring, when the reservoir tends to be full from winter rains and agricultural use is limited. Each lake and its basin was evaluated and investigated in order to carry out a modeling analysis of the surface erosion with the common models (RUSLE, MMF). These lakes are mainly used for irrigation of agricultural crops; however, some are used for sport fishing, forest-fire-fighting and other objectives. Table 1 shows the main characteristics of the basins corresponding to such lakes. Table 2 reports historical data regarding the lakes volume at the time of construction. The comparison between 2010 and 2018 is summarized in Table 3.



Figure 1. Lakes geographic distribution in Tuscany, Italy.

In order to implement the erosion estimation models (RUSLE and MMF), data for the hydrographic basins were collected relative to the precipitation (Figure 2) of the meteorological stations closest to the lakes; the hydrological network was elaborated, for each basin, from a DTM (Digital Terrain Model) with resolution 10×10 m (Figure 3); and land cover was processed via photointerpretation (Figure 4, Table 4) in 9 main classes.

Table 1. Main characteristics of the basins corresponding to the studied lakes (Appendix A): Altitude and slope are obtained from a DTM with 10 m resolution. Hydrographic networks are taken from a database of the regional administration of Tuscany (<https://www.regione.toscana.it/-/geoscopio>, accessed on 1 April 2018); viability is taken from the OpenStreetMap database.

GID	Lake Name	Area (ha)	Altitude Max (m agl)	Altitude Lake (m agl)	Slope Mean (%)	Hydrographic Network (m)	Road Network (m)
1156	Romena	9.55	293	154	15.1	618.8	331.5
2629	Cavalcanti	61.64	212	156	10.9	2594.6	751.4
3036	Galliano	67.25	409	281	8.3	3515.7	2883.1
5171	Fabbrica	218.99	413	229	14.1	11,268.2	11,812.8
7438	Pavone	50.83	202	135	14.4	1998.9	1029.9
7719	Schifanoia	87.04	281	242	4.6	4549.5	2297.4
8454	Castelfalfi 1	52.70	261	158	14.8	2459.3	4034.4
8477	Castelfalfi 3	127.19	177	99	10.3	7852.2	6069.4
8967	Potenti 2	65.34	183	48	11.5	4135.1	1091.1
8969	Potenti 1	43.79	128	39	9.4	2351.5	0.0
11525	Angiola	136.16	195	35	14.6	8183.8	11,074.5
12964	Castelfalfi 2	64.00	338	177	17.5	3507.2	1476.0

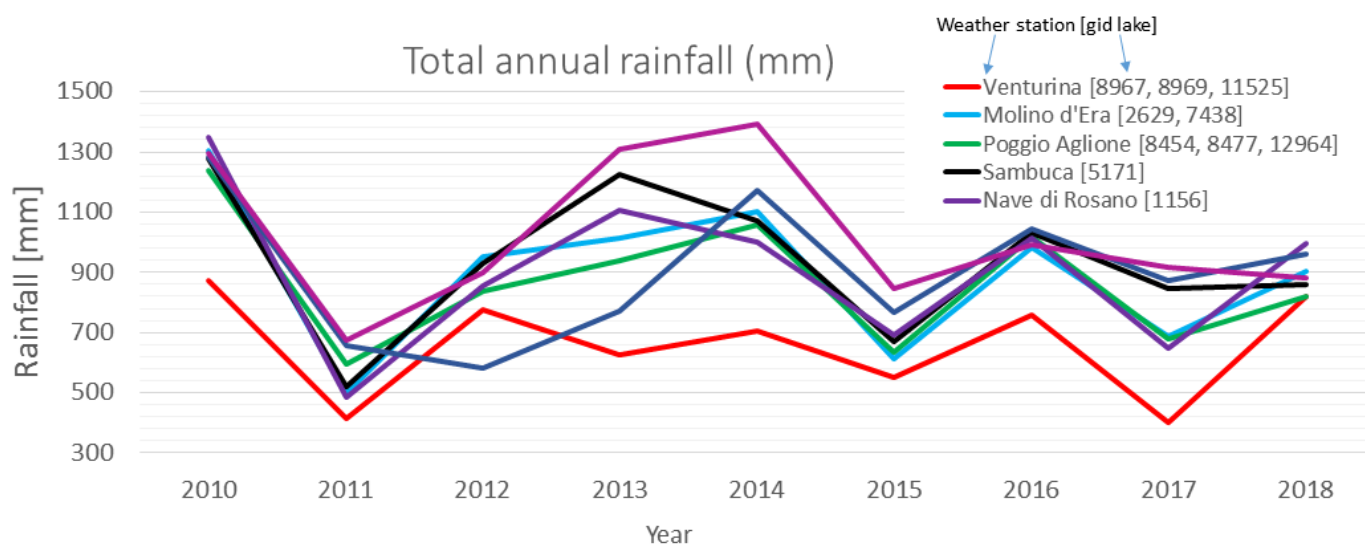


Figure 2. Rainfall trends in the period object of study, for the nearest weather stations. The legend on the right side associates each weather station to the corresponding lake(s).

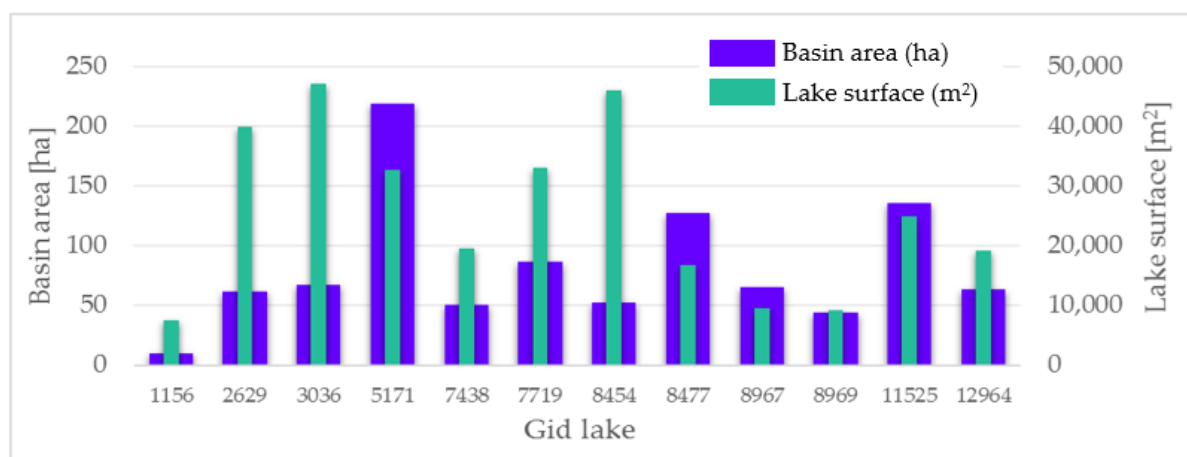


Figure 3. Relationships between lake surface and corresponding drainage basin.

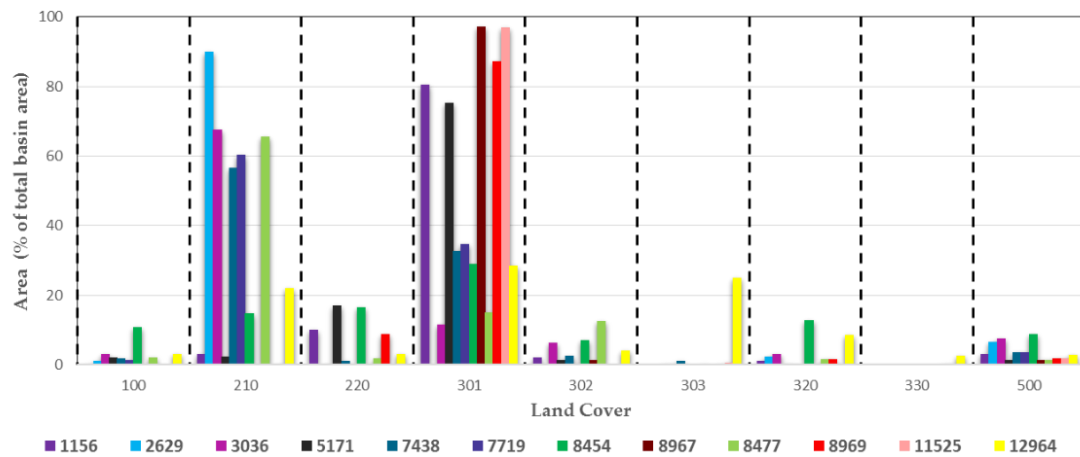


Figure 4. Distribution of land-cover classes for each lake. The land-use classes are shown along the x axis, described in Table 4, while the legend shows the lake GID. In X axis: 100 = artificial surfaces; 210 = lands under a rotation system used for annually harvested plants and fallow lands; 220 = permanent crops (vineyards and olive groves); 301 = forest with a complete canopy closure or a little less; 302 = forest with a sparse canopy closure (40–60%), shrubs and max 10% of soil bare; 303 = degraded forest (canopy closure less of 40%), shrubs cover of 40% and bare soil max 30%; 320 = permanent shrub and/or herbaceous vegetation associations; 330 = degraded soil or bare rock; 500 = water bodies.

From research conducted in the archives of the body in charge of the regulation and authorization of artificial lakes, it was also possible to recover the lake volume on the project deposited during the authorizations phase. From what has been learned, however, unregistered changes have often occurred regarding the morphology of the reservoir, so the related dimensional parameters are to be considered just indicative (Table 2, Figure 5).

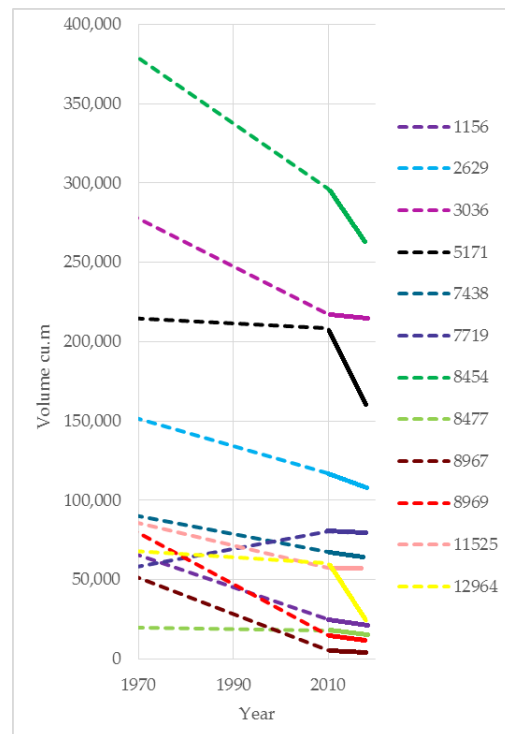


Figure 5. Trend of the reservoir capacity from construction to the analysis period. Dashed lines indicate the uncertain range, while solid lines indicate the trend found with the actual analysis.

Table 2. Construction year and project volumes.

GID	Construction Year	Volume of Design Phase (mc)
1156	1964	76,000
2629	1958	160,000
3036	1958	293,150
5171	1956	216,420
7438	1959	96,000
7719	1970	52,500
8454	1970	400,000
8477	1963	20,507
8967	1970	63,000
8969	1970	96,000
11525	1970	93,000
12964	1967	69,803

Table 3. Lake parameters for the years 2010 and 2018: surface area, volume, variation (in volume, percentage and percentage per year), and silting rate, the latter normalized to the lake surface area. For 2010, we show harmonized volumes, indicated as 2010 h.

GID	Surface (m ²)		Volume (m ³)		Variation			Silting	
	2010	2018	2010-h	2018	m ³	%	%/y	Mg	Mg/y
1156	7570	7599	24,855	21,597	−3258	−13.1	−1.6	2821	353
2629	38,875	39,942	116,826	108,254	−8572	−7.3	−0.9	7423	928
3036	49,986	47,241	217,520	215,144	−2376	−1.1	−0.1	2057	257
5171	35,293	32,713	208,807	159,454	−49,353	−23.6	−3.0	42,740	5342
7438	20,729	19,561	67,659	64,228	−3431	−5.1	−0.6	2971	371
7719	35,080	33,029	80,651	79,407	−1244	−1.5	−0.2	1077	135
8454	48,412	46,044	296,296	261,833	−34,463	−11.6	−1.5	29,845	3731
8477	13,389	16,747	18,018	15,315	−2703	−15	−1.9	2341	293
8967	8059	9654	5792	4141	−1651	−28.5	−3.6	1430	179
8969	7744	9180	15,220	12,070	−3150	−20.7	−2.6	2728	341
11525	21,246	24,886	57,625	57,238	−387	−0.7	−0.1	335	42
12964	22,135	19,204	60,549	23,953	−36,596	−60.4	−7.6	31,692	3961

Table 4. Land cover classes corresponding to C and P factors.

UCS Code	Description	USLE_C	USLE_P
100	Artificial surfaces	0	1
210	Lands under a rotation system used for annually harvested plants and fallow lands	0.15	1
220	Permanent crops (vineyards and olive groves)	0.4	1
301	Forest with a complete canopy closure or a little less	0.01	1
302	Forest with a sparse canopy closure (40–60%), shrubs and max 10% of soil bare	0.08	1
303	Degraded forest (canopy closure less of 40%), shrubs cover of 40% and bare soil max 30%	0.20	1
320	Permanent shrub and/or herbaceous vegetation associations	0.1	1
330	Degraded soil or bare rock	0.75	1
500	Water bodies	0	1

Harmonization

In order to compare the two volume measures, a lake-surface-based harmonization was applied, as this parameter (surface area) was easily obtained from the Tuscany Region orthophotos at 20 cm resolution (<https://www.regione.toscana.it/-/geoscopio>, accessed on 1 April 2018). Harmonization is necessary because in two different years we could have a different reservoir capacity due to the water level, according to different previous rainfall. It is based on the surface variation between 2010 and 2018 (Figure 6), according to the following equations.

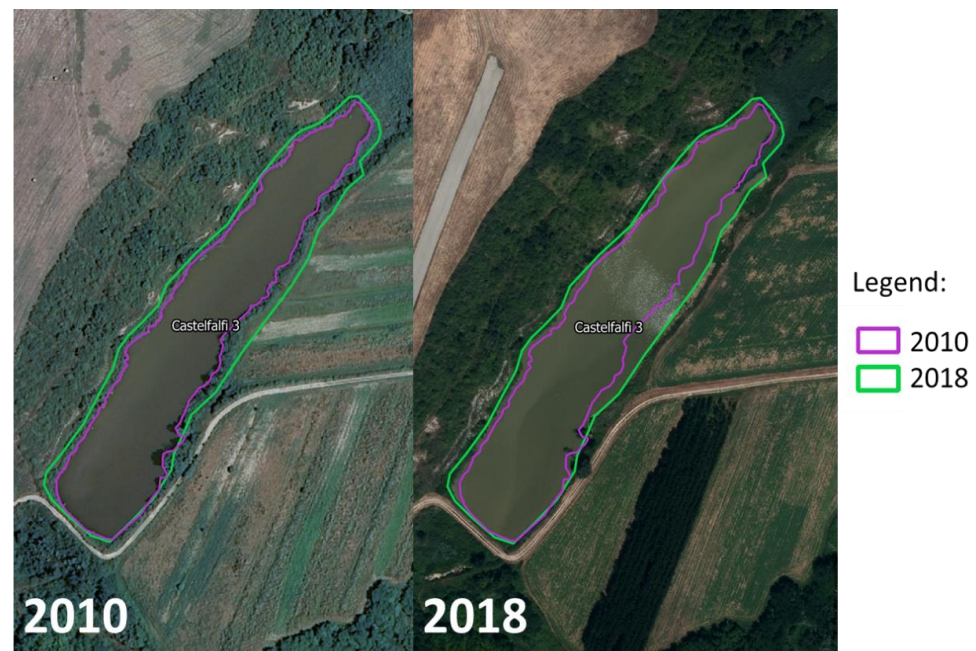


Figure 6. Orthophotos of lake “gid 8477” where it is possible to check the difference in water level.

We can write a generic expression for the lake volume V , according to Giambastiani [57], as:

$$V = \iint h(x, y) \cdot dx dy = \int_S h \cdot d\sigma \quad (1)$$

where h is the height that depends on the coordinate positions (x, y) , which we have omitted in the second step, rewriting the integral as a surface one (σ). Using the integral mean value theorem, we can write V as:

$$V = \langle h \rangle_S \cdot S \quad (2)$$

$\langle h \rangle_S$ being the lake height average (over the surface S). If we assume that its variation is negligible for limited variation of S , we can write the variation ΔV of the volume as a linear function of ΔS , the latter being the variation of the surface with time (depending for instance to rainfall, evaporation, etc.).

$$\Delta V = \langle h \rangle_S \cdot \Delta S = \underline{h} \cdot \Delta S \quad (3)$$

The last step is just to rename $\langle h \rangle_S$ with \underline{h} , both for simplicity and to highlight the assumption that it is no more dependent on the surface extension S .

In practice, we have measured \underline{h} for the reference year y_0 , which for us was the year 2010, for which we had the ARSIA measurements of the surface areas with the corresponding volumes.

Where the “Surface measured 2010” is the ARSIA surface, measured simultaneously with the volume

$$\underline{h} = \frac{V_{y_0}}{S_{y_0}} \quad (4)$$

For a generic year y , the volume to be compared with the one at the reference year y_0 becomes:

$$V_y = V_{y_0} + \Delta V = V_{y_0} + \underline{h} \cdot \Delta S \quad (5)$$

with ΔS as the surface difference between 2018 and 2010; surfaces were obtained through photointerpretation of orthophotos.

2.2. Erosion Simulation by the Morgan–Morgan–Finney Model

The MMF model divides the soil erosion process into two phases: the phase related to the water component, which determines the energy of the rainfall, and the phase related to the production of sediments, based on the characteristics of the soil. Soil loss in relation to erosion is determined on the basis of precipitation and transport capacity, influenced by soil cover and slope [41,59]. The MMF model is implemented within the open-source SAGA GIS software. Input data come from various sources. Starting from the Digital Terrain Model (DTM), with a resolution of 10 m, the slope map and the channel network were elaborated, while the “plant height” map was obtained through the Crown Height Model (CHM—10 × 10 m). Canopy cover, permanent interception and ground cover derive from Sentinel-2 image processing, in particular based on the NDVI calculation [60], with 10 m resolution. The characteristics of the soils (bulk density, effective hydrological depth, percentages of clay, sand and silt, etc.) are derived from the soil database of RT (<http://www502.regione.toscana.it/geoscope/pedologia.html>, accessed on 1 April 2018). Other necessary input variables for the model were obtained from direct processing of the land use and land cover map, carried out by photointerpretation. Annual precipitation data were taken from the meteorological stations closest to the lakes in question. In particular, the average distance between the lakes and the rain gauges is 4.5 km, with a standard deviation of 1.8 km.

2.3. Erosion Estimate by RUSLE Model

The Universal Soil Loss Equation (USLE) [23] and subsequent revisions (RUSLE) [24], is an empirical relationship, as it derives from experimental plots carried out in the United States and from the mathematical definition of the results found from these plots, which models soil erosion as a process resulting from a set of six main factors: the energy and intensity of precipitation (R factor), the erodibility of the soil (K factor), the length and slope of the plot (LS factor), vegetation cover (C factor) and conservation practices (P factor). The employed R factor is derived from the SIAS project (ISPRA 2016), through which a simplified relationship is elaborated between the amount of rainfall and the erosion value [61]. This simplification does not critically affect the accuracy, as it emerges from comparison work [31]. In fact, the mean value of R factor for Tuscany is 1765 (standard deviation = 710) against 1748 (standard deviation 365), as found by Panagos 2015 [29]. Larger fieldwork, developed in 2006 for punctual soil data, allowed the calculation of K factor carried out following the original methodology [23]. The LS factor was calculated for the basins of each lake, using a digital elevation model (DEM) of 10 × 10 m, with the method developed by Desmet and Govers 1996 [62]. In order to avoid overestimation of the LS factor in heterogeneous landscapes, the lengths of long slopes were limited to a value of 333 m [24,62]. The length exponent (m) is based on the original USLE method [63]. The C factor was completely updated, carrying out a detailed photo interpretation on orthophotos, using functional classes for the purpose. For each soil cover class identified, the values C and P were attributed as in Table 4, consistent with the values reported in the bibliography [24,31,64,65].

From the photo interpretation, it was possible to verify that in the agricultural landscapes of the study areas, there were no particular conservation techniques similar to those already codified in the RUSLE model: for this reason, we decided to always adopt a factor P = 1.

Sediment Delivery Ratio

The Sediment delivery ratio (SDR) is applied to estimate the amount of sediments produced by the erosion phenomena that reaches the lake [66]. SDR is the erosion fraction, generated by each single source cell, which reaches the nearest permanent drainage line. As a first approximation, the SDR can be considered constant for the whole basin or sub-basin [67], but in recent works, it is calculated pixel by pixel as a function of the length and slope of the path in the downstream direction [68]. The most complete al-

gorithm for its modeling is proposed by [65], which accounts for the connectivity index (IC) for each pixel, considering the morphological and hydrological characteristics of both the hydrological upstream and downstream portion of the pixel. It describes the hydrological link between sediment sources and collection and transfer points such as streams [69]. For SDR calculation in the study area, we have used the InVEST model (<https://naturalcapitalproject.stanford.edu/>, accessed on 3 September 2021), which implemented the algorithm of Borselli [65], making some minor simplifications.

3. Results

The silting rate (SR) (Figure 7) is very variable among the lakes under study and no significant relationships appear between the lake volume or the surface of the basin, or other main dimensional parameters. Some lakes have a high volume variation (e.g., 12964, 5171) and this is not related to either the size of the lake or the basin. The annual silting rate is obtained by dividing the volume variation by 8. We consider this operation significant as the surveys were carried out, in both cases, during the months of March and April, with a difference of a few weeks. The lakes' surfaces did not vary much during the 8 years of analysis. Figure 8a shows the relationship between the area of 2010 and 2018. The strong correlation indicates that the variation in the surface responds to ordinary dynamics. The surface change is present in almost all lakes; from this, we can confirm the need to harmonize volumes. While this process may be the source of further processing errors, we believe it is robust as the volume variations are small. A greater variation may exist in the relationship between the lakes' mean depths (Figure 8b). For all cases, we found that the mean depth has decreased. This is further confirmation of the soundness of the harmonization process. The correlation matrix highlights significant relationships between several parameters considered (Figure 9). Among these, we find a good correlation between soil loss and the erodibility of the lithology (K_{lito_SL} , $r = -0.72$), the quantity of specialized (olive grove, vineyard) agricultural land cover ($r = 0.85$) and with the presence of roads ($r = 0.68$).

In Figure 9, we summarize the many relationships developed between the silting and the characteristics of the lake or basin. Among these are the physical characteristics of the basin, such as the altimetry and the difference in height (alti-max and altit_lake, disl_basin), the length of the network present in the basin (hydro_network), the presence of roads (road_net), the various soil classes (sup_ucs: Table 4) and rainfall (rain_acc, num_event).

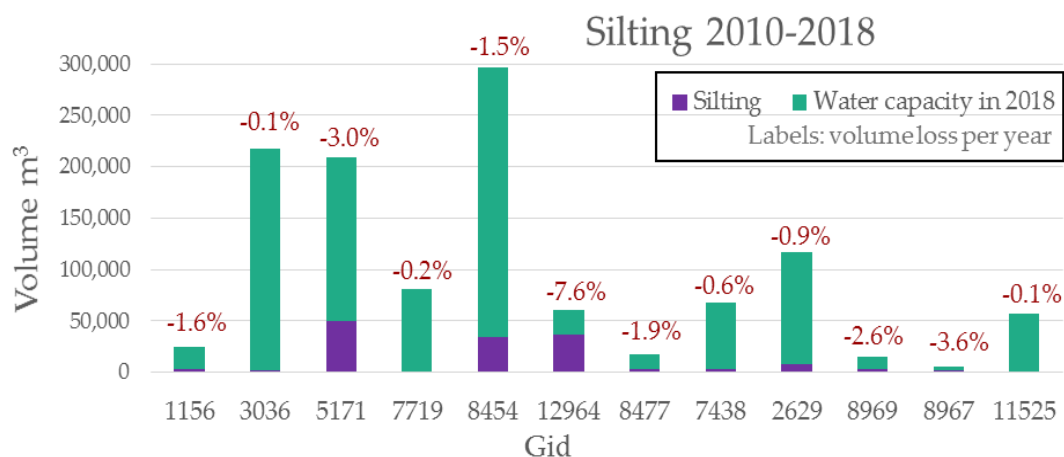


Figure 7. Silting rate and water capacity of the lakes under study.

Comparing the silting rate (SR) of each lake, obtained with the proposed methodology [57], with the annual soil-loss values obtained from the described empirical models, the link between these methodologies is evident (Figure 10). In absolute terms, the sediment values produced (SL) were almost always lower than the SR values. SL by RUSLE was similar to SR for three lakes. In seven cases, however, it was different, even if it was

consistent with the MMF results. For example, Lake 5171 had the highest silting rate with 3701 Mg y^{-1} , which was similar to the MMF estimate (3384), while with RUSLE, we found a third of the soil was lost. It should be noted that this lake has a much larger basin than all the others. Lake 8477 showed an inverse and very different trend compared to the models: 202 (SR), 630 (SL-RUSLE), 675 (SL-MMF). For other lakes, we found a close similarity. For example, lake 2629 had SR = 643; RUSLE = 499; MMF = 558 Mg y^{-1} . Additionally, in statistical terms, SR showed higher absolute values (SR/ha mean = 15.1; SL MMF/ha mean = 7.9; SL RUSLE/ha mean = 6.3).

Using the RUSLE and SAGA MMF models, it was possible to estimate the soil-loss rate of each catchment area [70], which was compared with the average silting rate of the reservoirs (considered as the closure section of the basin), in the period 2010–2018. The average sediment produced per hectare for the entire analysis sample was in line with the work of Angeli et al. 2004 [71]. The average annual soil loss per hectare obtained by RUSLE was 6.35 Mg, while MMF returned 7.96 Mg. The average silting per hectare of catchment area was 15.13 Mg y^{-1} (Table 5). Both models showed a good correlation with the silting rate measured for each lake (Figure 11), but with a stronger relationship with the RUSLE model. The good significance of such relationships suggests a close link between the loss of soil and the silting rate, as visible in Figure 10.

Table 5. Summary of sediment volumes and average values per hectare, obtained from field surveys (silting) and models (soil loss for RUSLE and MMF).

GID Lake	Basin Area (ha)	Silting (Mg/y)	SL RUSLE (Mg/y)	SL MMF (Mg/y)	Silting ($\text{Mg y}^{-1} \text{ ha}^{-1}$)	RUSLE ($\text{Mg y}^{-1} \text{ ha}^{-1}$)	MMF ($\text{Mg y}^{-1} \text{ ha}^{-1}$)
1156	10	244	49	4	24.393	4.928	0.422
2629	60	643	499	559	10.703	8.306	9.299
3036	81	178	344	609	2.197	4.242	7.511
5171	213	3701	1248	3384	17.390	5.862	15.900
7438	50	257	290	871	5.183	5.842	17.543
7719	101	93	192	7	0.925	1.899	0.071
8454	41	2585	655	721	63.529	16.092	17.733
8477	106	203	630	675	1.906	5.925	6.349
8967	53	124	11	3	2.341	0.209	0.049
8969	32	236	17	3	7.329	0.523	0.088
11525	135	29	31	1	0.215	0.229	0.004
12964	60	2745	1342	1247	45.475	22.231	20.653

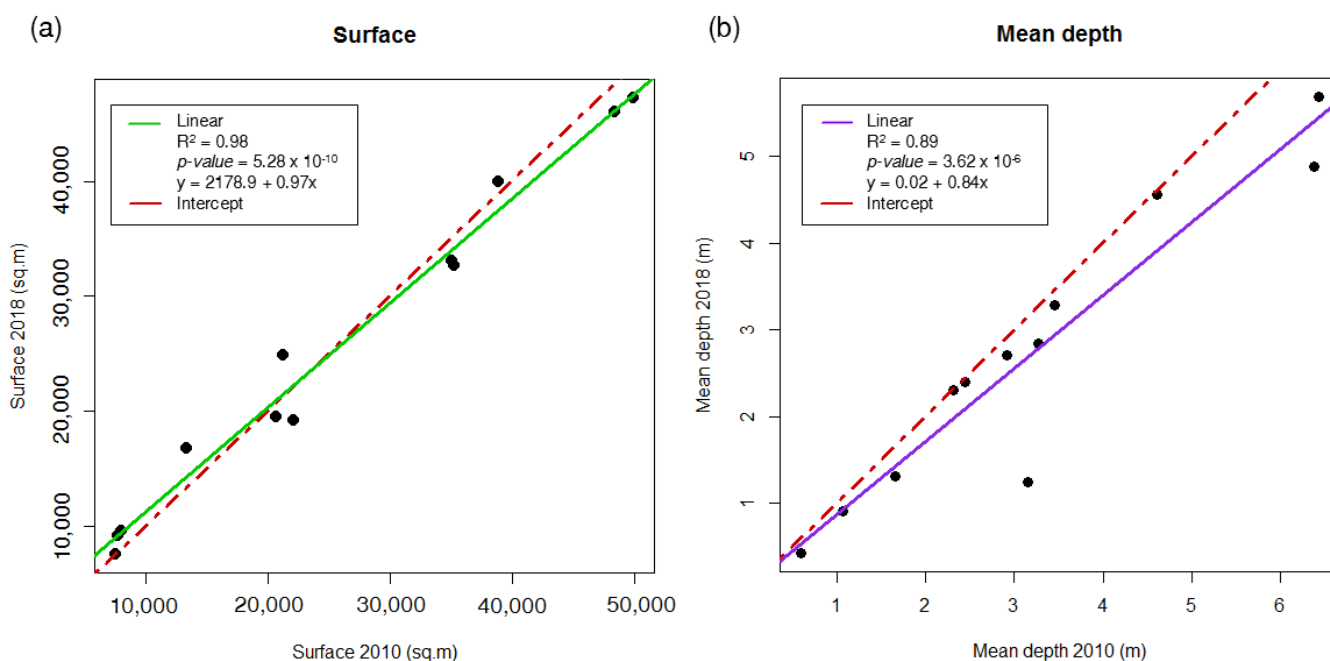


Figure 8. Relationships between variations in surface area (a) and mean depth (b).

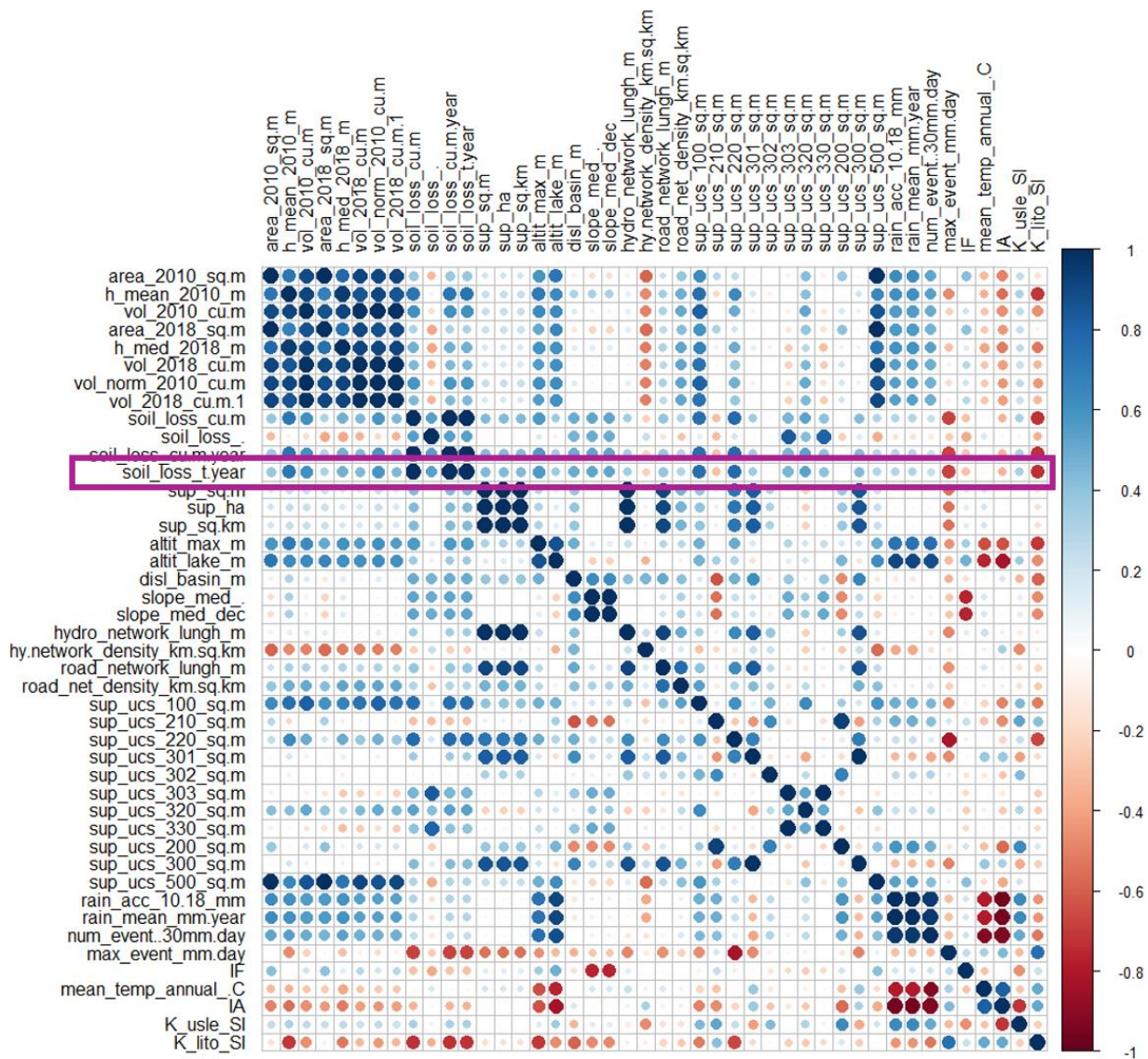


Figure 9. Correlation matrix, based on Pearson’s analysis.

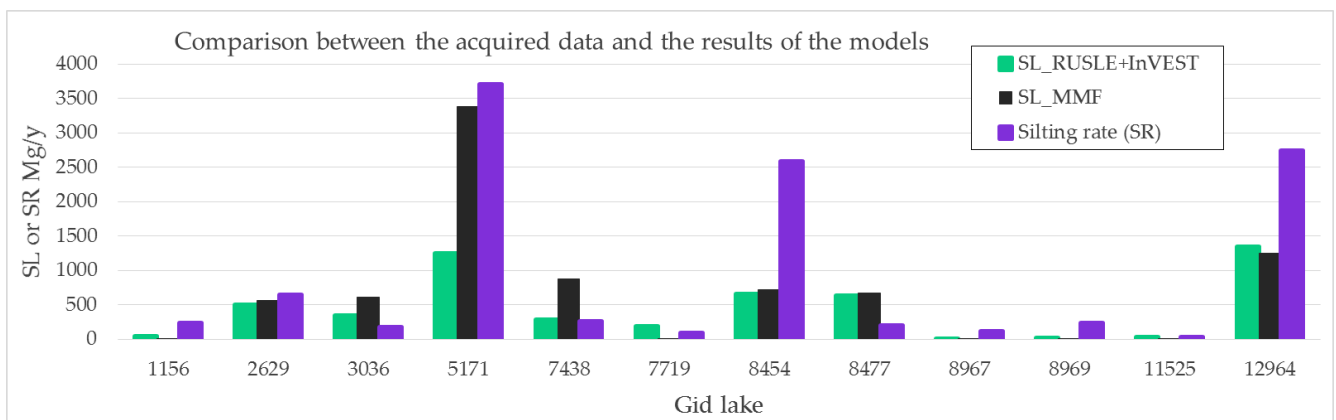


Figure 10. Comparison between the soil loss (SL) calculated with the models (RUSLE and MMF) and the silting rate for each individual lake.

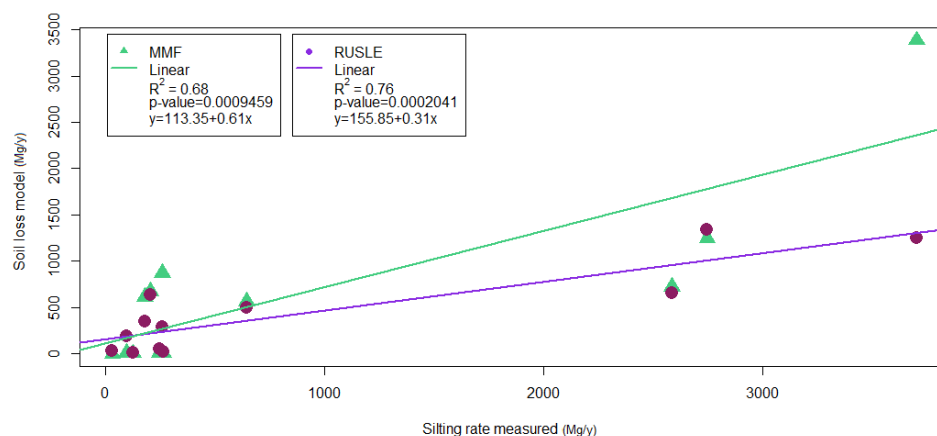


Figure 11. Relationship between the measured silting rate and the soil loss obtained from the MMF and RUSLE models.

4. Discussion

The methods that allow the monitoring of erosive phenomena are often very expensive to apply: the models require several input variables and therefore (I) challenging surveying campaigns, (II) data collection from different sources to be harmonized and (III) aerial images and high-resolution digital terrain models for GIS analysis and photointerpretation. All this involves high costs, low reaction time in carrying out analyses at critical moments, and possible relevant evaluation errors due to the high number of interactions and variables to take into account [4]. The proposed approach for the erosion evaluation is based on monitoring the water capacity of hilly lakes, which are considered as real sediment containers. The variation in lake volume, following silting, can be linked to the production of sediments from the afferent basin. Given the high distribution of artificial hilly reservoirs in the Tuscan territory, the proposed approach could create conditions for a periodic assessment of the degradation phenomena of the soil and the territory in general. The use of input data with greater accuracy and precision, such as using LiDAR Dems [70] and an in situ meteorological station for precipitation measurements, could lead to improvements. This approach is also easily applicable to different contexts, as long as they have a good distribution of hilly reservoirs. The methodology, however, has some limitations for calculating the volume of the lake, in particular due to the simplification of the shape of the lake profile [57]. Anyway, the application of this methodology, from a monitoring point of view, can be valuable for reducing major evaluation errors arising from too-long sampling-time intervals that we have when using classical approaches. In fact, field measurements for medium-sized reservoirs (up to 4–5 hectares of surface area) can be carried out in a short time (e.g., 30 min), and processing can be carried out automatically within a few minutes. This allows a wide and rapid application, analyzing wide domains with relatively low effort and costs. The results obtained show significant measures of the lake volume variation, well correlated with other physical lake variables. The comparison of the mean depth between 2010 and 2018 (Figure 8) shows a very strong relationship ($R^2 = 0.89$ and $p\text{-value} = 3.619 \times 10^{-6}$), which indicates a good significance of the methodology. Furthermore, the values are located below the bisector, as in no case do we find negative silting (greater lake depth). This leads us to think further that the methodology is correct. Given the small variation in terms of volume in most cases (Figure 7), calculation errors, however accepted, could lead to mathematical anomalies. Mathematical models verify the physical process of sediment accumulation in the lake. The 12 basins analyzed are very different from each other (average surface = 78 ± 54 hectares); they mainly have soil covers relating to arable land and forest, so with high variability. We also found evident differences in terms of precipitation. The lakes examined are well distributed and are representative enough of the study area, Tuscany. Some lakes exhibit very high-volume variations (Figure 7). For example, Lake 12964 has a silting rate of 45 tons/year per hectare of basin.

Close to the lake, we found a pig farm on an area of about seven hectares, a practice that has probably greatly affected erosion. Lake 5171 has the largest basin of all the lakes under study, with a greater total length of variability, another important source of sediment when maintenance is limited. Lake 8454 also has a strong silting; in this case, the data available do not show any trend and the lack of knowledge of the specific territory does not allow us to put forward hypotheses. Lake 11525 has a silting rate of 0.21 ton/year per hectare of basin, and has the basin completely covered by forest. The models used provided data compatible with the results of other authors [34,40]. The soil-loss values obtained from the basins show a significant correlation with the silting rate values (Figure 10), regardless of the intrinsic great variability. In some cases, soil loss is greater than the volume variation (8 out of 24, Table 5); in particular, this concerns large basins (about 100 hectares). One reason can be that the sediment produced by the basin does not reach the lake. Another factor that has not been taken into account concerns the suspended sediment lost by the reservoir spillway. Tauro [72] indirectly estimates suspended solids by means of water turbidity. The concentration of suspended solids typically increases with the flow speed. In a lake, the effect of containment and slowdown of the outflows allows greater sedimentation. In fact, the water flowing in the spillways usually appears clear [73]. The opposite behavior occurs in smaller basins (less than 50 hectares), which are characterized by higher silting rates and lower soil loss values. The actual erosion is caused by phenomena that, in some cases, the models are unable to consider, which concern the slopes closest to the lake (such as the case of the lake with pig breeding). Having such present shortcomings in mind, the applied methodology can be useful for building decision-support systems in spatial planning and monitoring areas that show critical characteristics related to hydrological processes [74].

5. Conclusions

A new approach for the soil erosion analysis was proposed. It consists of the use of an aquatic boat bringing a GPS sonar. In few minutes, it is able to detect data about water depth in the reservoir. Using an automatic GIS process, it is possible to obtain an estimation of the volume. The methodology was applied to 12 hilly lakes mainly for irrigation purposes, for which the volume (or reservoir capacity) was measured and repeated after 8 years, using comparable instruments (sonar with GPS). The volume variation in this period was compared with soil-loss estimates obtained from well-established models widely known in the scientific community (RUSLE and MMF), obtaining a clear relationship between the two variables. This approach allows low-cost monitoring of the soil erosion phenomena in relation to changes in land use or climate change. Being based on lakes, the analysis can refer to specific portions of the territory. The main advantage is the speed of carrying out the survey on the lake; the instrumentation is inexpensive and it is not necessary to acquire other parameters relating to the basin. The processing procedure can be automated in the GIS environment. The method can be applied to land management issues as a tool for a decision-support system. The harvesting of more data could permit the development of some estimate models about the erosion phenomena based on the silting rate of lakes.

Author Contributions: Conceptualization, S.C. and R.G.; methodology, L.G. and S.C.; software, L.B. and S.R.; validation, R.G. and M.I.; formal analysis, Y.G. and L.G.; investigation, Y.G., R.G., S.C.; resources, B.G. and A.O.; data curation, Y.G.; writing—original draft preparation, Y.G.; writing—review and editing, A.O., S.C. and R.G.; visualization, M.I.; supervision, L.B. and A.O.; project administration, B.G.; funding acquisition, B.G. and L.B. All authors have read and agreed to the published version of the manuscript.

Funding: This research was carried out with the ordinary funds of the LaMMA Consortium and CNR-IBE and with external funding from the Tuscany Region: Decrees 100/2018 and 1345/2018 “Mappatura della totalità dei laghi in Regione Toscana e costituzione del catasto informatizzato”.

Institutional Review Board Statement: Not applicable.

Informed Consent Statement: Informed consent was obtained from all subjects involved in the study.

Data Availability Statement: Not applicable.

Acknowledgments: The data used for this article derive from the hilly lakes census of the Tuscany Region.

Conflicts of Interest: The authors declare no conflict of interest.

Appendix A



Figure A1. Castelfalfi lakes and basins. GID: 8454 = Castelfalfi 1; 12964 = Castelfalfi 2; 8477 = Castelfalfi 3.

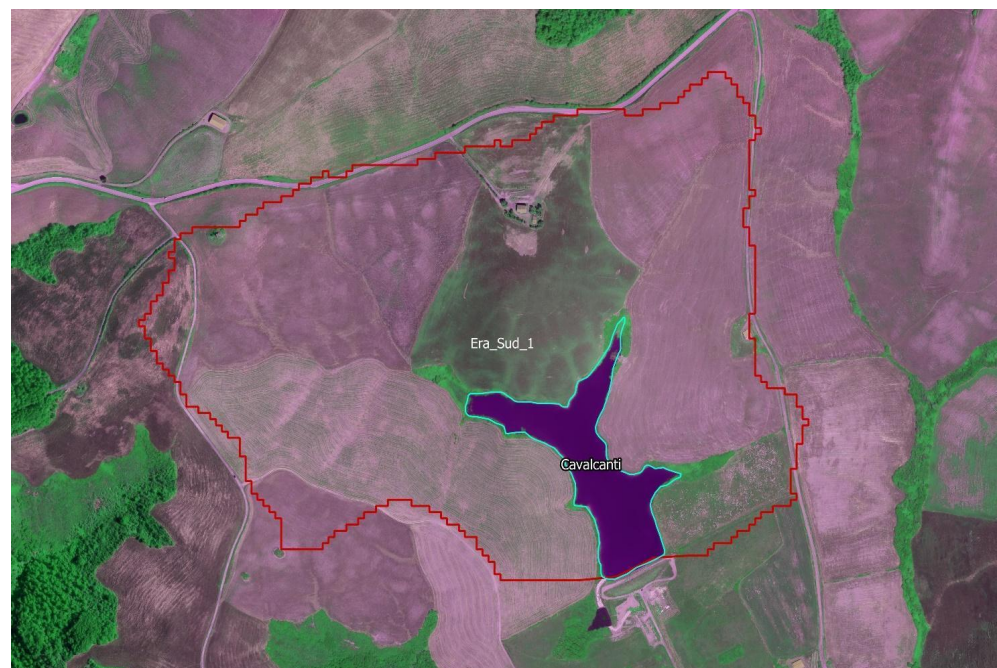


Figure A2. Cavalcanti lake and basin. GID: 2629.



Figure A3. Fabbrića lake and basin. GID: 5171.

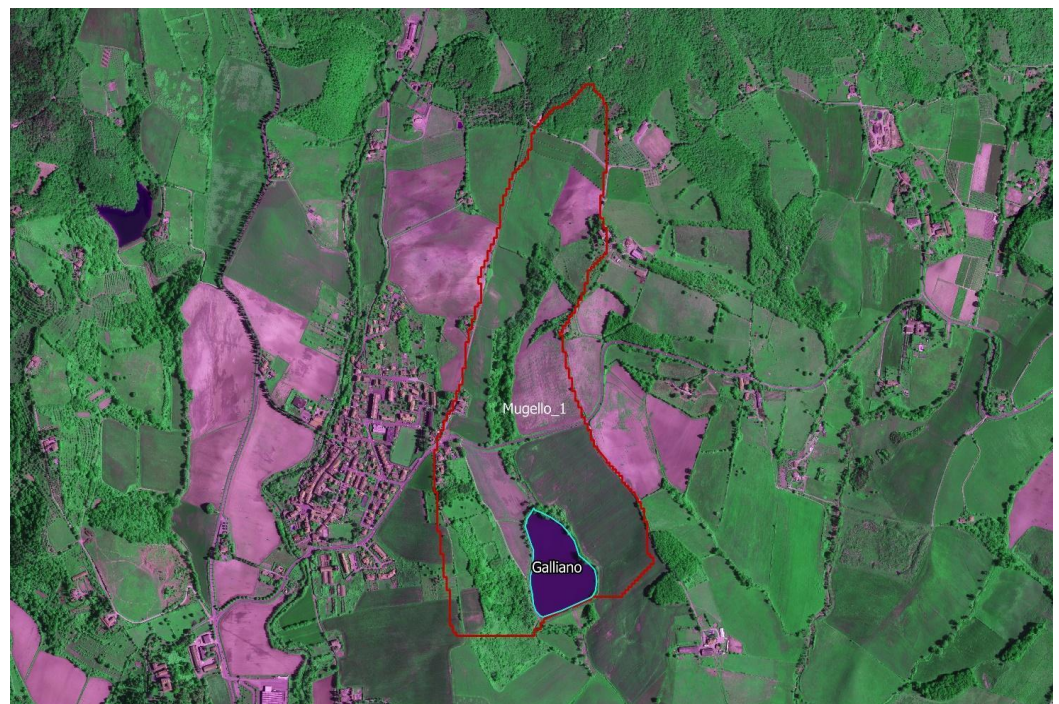


Figure A4. Galliano lake and basin. GID: 3036.



Figure A5. Pavone lake and basin. GID: 7438.



Figure A6. Romena lake and basin. GID: 1156.

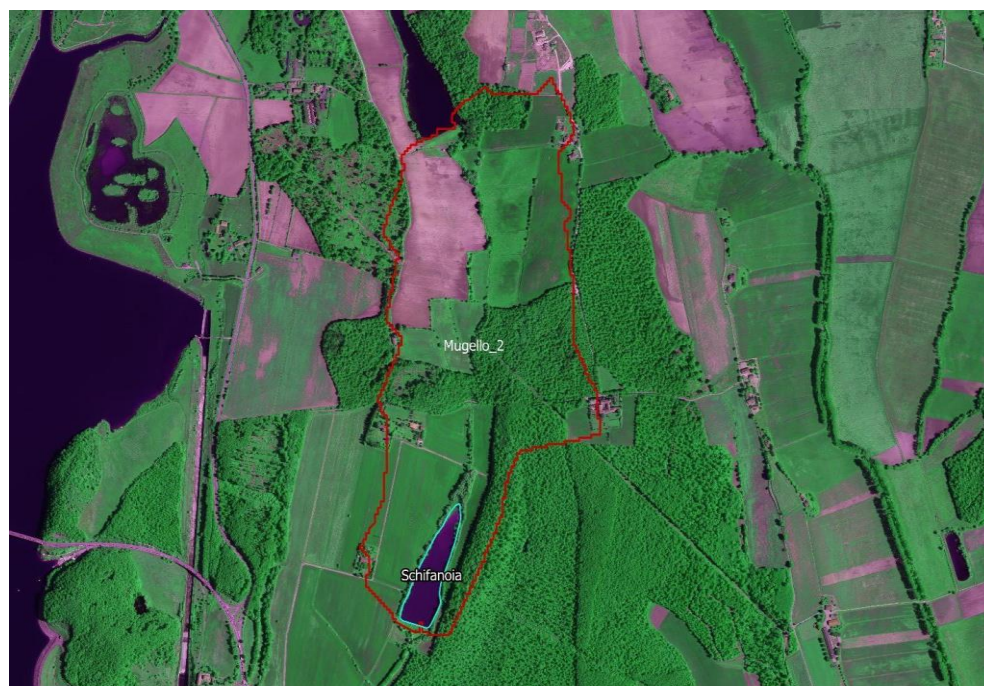


Figure A7. Schifanoia lake and basin. GID: 7719.

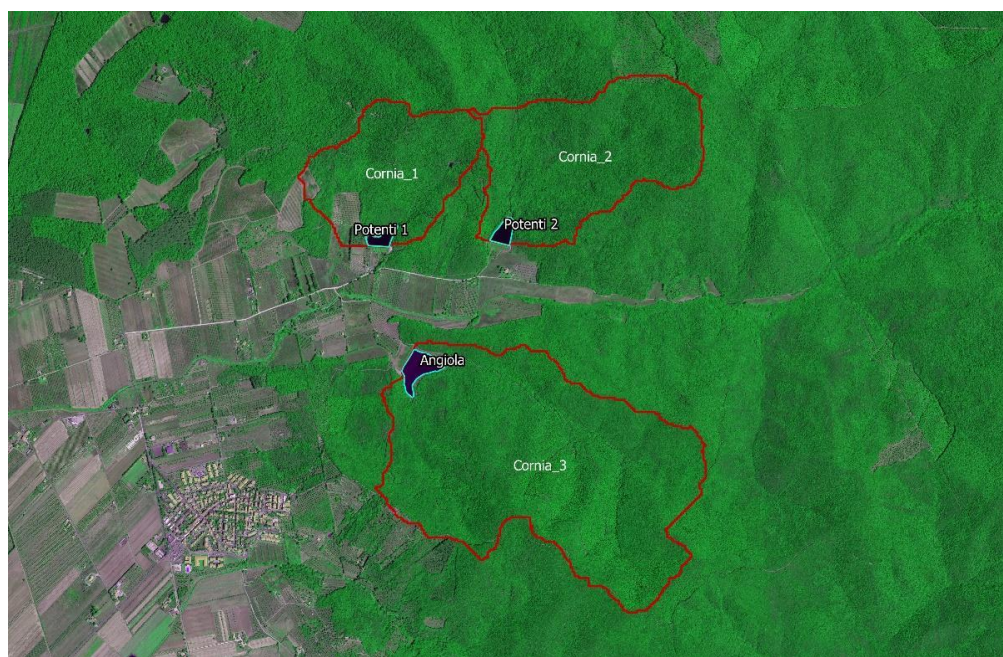


Figure A8. Cornia lakes and basins. GID: 8969 = Potenti 1; 8967 = Potenti 2; 11525 = Angiola.

References

1. Borrelli, P.; Robinson, D.A.; Panagos, P.; Lugato, E.; Yang, J.E.; Alewell, C.; Wuepper, D.; Montanarella, L.; Ballabio, C. Land use and climate change impacts on global soil erosion by water (2015–2070). *Proc. Natl. Acad. Sci. USA* **2020**, *117*, 21994–22001. [[CrossRef](#)]
2. Pimentel, D. Soil erosion: A food and environmental threat. *Environ. Dev. Sustain.* **2006**, *8*, 119–137. [[CrossRef](#)]
3. Pimentel, D.; Burgess, M. Soil erosion threatens food production. *Agriculture* **2013**, *3*, 443–463. [[CrossRef](#)]
4. Pennock, D.; Pennock, L.; Sala, M. *Soil Erosion: The Greatest Challenge for Sustainable Soil Management*; Food & Agriculture Organization: Rome, Italy, 2019; ISBN 9789251314265.
5. Pimentel, D.; Harvey, C.; Resosudarmo, P.; Sinclair, K.; Kurz, D.; McNair, M.; Crist, S.; Shpritz, L.; Fitton, L.; Saffouri, R.; et al. Environmental and economic costs of soil erosion and conservation benefits. *Science* **1995**, *267*, 1117–1123. [[CrossRef](#)] [[PubMed](#)]

6. Kirkby, M.; Jones, R.J.; Irvine, B.; Gobin, A.G.G.; Cerdan, O.; van Rompaey, J.J.; Huting, J.R.M. *Pan-European Soil Erosion Risk Assessment for Europe: The PESERA Map, version 1 October 2003*; Office for Official Publications of the European Communities: Luxembourg, Germany, 2004.
7. Nearing, M.A.; Foster, G.R.; Lane, L.J.; Finkner, S.C. A process-based soil erosion model for USDA-Water Erosion Prediction Project technology. *Trans. ASAE* **1989**, *32*, 1587–1593. [[CrossRef](#)]
8. Laflen, J.; Lane, L.; Foster, G.R. WEPP: A new generation of erosion prediction technology. *J. Soil Water Conserv.* **1991**, *46*, 34–38.
9. Assennato, F.; Antona, M.D.; Di Leginio, M.; Strollo, A. Assessing land consumption impact on ecosystem services provision: An insight on biophysical and economic dimension of loss of erosion control in Italy. *Authorea* **2020**, 1–12. [[CrossRef](#)]
10. Mastrorosa, S.; Crosetto, M.; Congedo, L.; Munafò, M. Land consumption monitoring: An innovative method integrating SAR and optical data. *Environ. Monit. Assess.* **2018**, *190*, 588. [[CrossRef](#)]
11. Van Oost, K.; Bakker, M. Soil Productivity and Erosion. *B Soil Ecol. Ecosyst. Serv.* **2012**, *2012*, 301–314. [[CrossRef](#)]
12. Stokes, A.; Douglas, G.B.; Fourcaud, T.; Giadrossich, F.; Gillies, C.; Hubble, T.; Kim, J.H.; Loades, K.W.; Mao, Z.; Mcivor, I.R.; et al. Ecological mitigation of hillslope instability: Ten key issues facing researchers and practitioners. *Plant Soil* **2014**, *377*, 1–23. [[CrossRef](#)]
13. Fox, D.M.; Laaroussi, Y.; Malkinson, L.D.; Maselli, F.; Andrieu, J.; Bottai, L.; Wittenberg, L. POSTFIRE: A model to map forest fire burn scar and estimate runoff and soil erosion risks. *Remote Sens. Appl. Soc. Environ.* **2016**, *4*, 83–91. [[CrossRef](#)]
14. Capra, G.F.; Ganga, A.; Grilli, E.; Vacca, S.; Buondonno, A. A review on anthropogenic soils from a worldwide perspective. *J. Soils Sediments* **2015**, *15*, 1602–1618. [[CrossRef](#)]
15. SEC. Communication from the Commission to the Council, the European Parliament, the European Economic and Social Committee and the Committee of the Regions. In *Thematic Strategy for Soil Protection*; [SEC(2006)620], [SEC(2006)1165]; Communication from the Commission to the Council: Brussels, Belgium, 2006.
16. Borrelli, P.; Robinson, D.A.; Fleischer, L.R.; Lugato, E.; Ballabio, C.; Alewell, C.; Meusburger, K.; Modugno, S.; Schütt, B.; Ferro, V.; et al. An assessment of the global impact of 21st century land use change on soil erosion. *Nat. Commun.* **2017**, *8*, 2013. [[CrossRef](#)]
17. Caracciolo, C.; Napoli, M.; Porcù, F.; Prodi, F.; Dietrich, S.; Zanchi, C.; Orlandini, S. Raindrop Size Distribution and Soil Erosion. *J. Irrig. Drain. Eng.* **2012**, *138*, 461–469. [[CrossRef](#)]
18. Napoli, M.; Marta, A.D.; Zanchi, C.A.; Orlandini, S. Assessment of soil and nutrient losses by runoff under different soil management practices in an Italian hilly vineyard. *Soil Tillage Res.* **2017**, *168*, 71–80. [[CrossRef](#)]
19. Napoli, M.; Cecchi, S.; Orlandini, S.; Mugnai, G.; Zanchi, C.A. Simulation of field-measured soil loss in Mediterranean hilly areas (Chianti, Italy) with RUSLE. *Catena* **2016**, *145*, 246–256. [[CrossRef](#)]
20. Canuti, P.; Moretti, S.; Bazzoffi, P.; Rodolfi, G.; Zanchi, C. Soil erosion as a result of the man activity-geological environment relationship an example of quantitative evaluation in the mugello valley (Tuscany, Italy). *Bull. Int. Assoc. Eng. Geol. l'Assoc. Int. Géol. l'Ingénieur* **1986**, *33*, 109–114. [[CrossRef](#)]
21. Bagarello, V.; Iovino, M.; Elrick, D. A Simplified Falling-Head Technique for Rapid Determination of Field-Saturated Hydraulic Conductivity. *Soil Sci. Soc. Am. J.* **2004**, *68*, 66. [[CrossRef](#)]
22. Vacca, A.; Loddo, S.; Ollesch, G.; Puddu, R.; Serra, G.; Tomasi, D.; Aru, A. Measurement of runoff and soil erosion in three areas under different land use in Sardinia (Italy). *Catena* **2000**, *40*, 69–92. [[CrossRef](#)]
23. Wischmeier, W.; Smith, D. *Predicting Rainfall Erosion Losses: A Guide to Conservation Planning*; Agriculture Handbook (No. 537); United States Department of Agriculture: Washington, DC, USA, 1978; pp. 1–67.
24. Renard, K.G. *Predicting Soil Erosion by Water: A Guide to Conservation Planning with the Revised Universal Soil Loss Equation (RUSLE)*; Agriculture Handbook (No. 703); United States Department of Agriculture: Washington, DC, USA, 1997; p. 300.
25. Poesen, J.; Nachtergaele, J.; Verstraeten, G.; Valentin, C. Gully erosion and environmental change: Importance and research needs. *Catena* **2003**, *50*, 91–133. [[CrossRef](#)]
26. Renschler, C.S.; Harbor, J. Soil erosion assessment tools from point to regional scales—The role of geomorphologists in land management research and implementation. *Geomorphology* **2002**, *47*, 189–209. [[CrossRef](#)]
27. Kinnell, P.I.A. Event soil loss, runoff and the Universal Soil Loss Equation family of models: A review. *J. Hydrol.* **2010**, *385*, 384–397. [[CrossRef](#)]
28. Lu, H.; Prosser, I.P.; Moran, C.J.; Gallant, J.C.; Priestley, G.; Stevenson, J.G. Predicting sheetwash and rill erosion over the Australian continent. *Aust. J. Soil Res.* **2003**, *41*, 1037–1062. [[CrossRef](#)]
29. Panagos, P.; Borrelli, P.; Meusburger, K. A new European slope length and steepness factor (LS-factor) for modeling soil erosion by water. *Geosciences* **2015**, *5*, 117–126. [[CrossRef](#)]
30. Panagos, P.; Meusburger, K.; Ballabio, C.; Borrelli, P.; Alewell, C. Soil erodibility in Europe: A high-resolution dataset based on LUCAS. *Sci. Total Environ.* **2014**, *479–480*, 189–200. [[CrossRef](#)] [[PubMed](#)]
31. Panagos, P.; Borrelli, P.; Meusburger, K.; Alewell, C.; Lugato, E.; Montanarella, L. Estimating the soil erosion cover-management factor at the European scale. *Land Use Policy* **2015**, *48*, 38–50. [[CrossRef](#)]
32. Panagos, P.; Ballabio, C.; Borrelli, P.; Meusburger, K.; Klik, A.; Rousseva, S.; Tadić, M.P.; Michaelides, S.; Hrabalíková, M.; Olsen, P.; et al. Rainfall erosivity in Europe. *Sci. Total Environ.* **2015**, *511*, 801–814. [[CrossRef](#)]
33. Benavidez, R.; Jackson, B.; Maxwell, D.; Norton, K. A review of the (Revised) Universal Soil Loss Equation ((R)USLE): With a view to increasing its global applicability and improving soil loss estimates. *Hydrol. Earth Syst. Sci.* **2018**, *22*, 6059–6086. [[CrossRef](#)]

34. Alewell, C.; Borrelli, P.; Meusburger, K.; Panagos, P. Using the USLE: Chances, challenges and limitations of soil erosion modelling. *Int. Soil Water Conserv. Res.* **2019**, *7*, 203–225. [[CrossRef](#)]
35. Le Roux, J.J.; Newby, T.S.; Sumner, P.D. Monitoring soil erosion in South Africa at a regional scale: Review and recommendations. *S. Afr. J. Sci.* **2007**, *103*, 329–335.
36. Morgan, R.P.C.; Duzant, J.H. Modified MMF (Morgan–Morgan–Finney) model for evaluating effects of crops and vegetation cover on soil erosion. *Earth Surf. Process. Landf.* **2008**, *32*, 90–106. [[CrossRef](#)]
37. Sterk, G. A hillslope version of the revised Morgan, Morgan and Finney water erosion model. *Int. Soil Water Conserv. Res.* **2021**, *9*, 319–332. [[CrossRef](#)]
38. Li, C.; Qi, J.; Feng, Z.; Yin, R.; Guo, B.; Zhang, F.; Zou, S. Quantifying the effect of ecological restoration on soil erosion in china's loess plateau region: An application of the MMF approach. *Environ. Manag.* **2010**, *45*, 476–487. [[CrossRef](#)]
39. Tesfahunegn, G.B.; Tamene, L.; Vlek, P.L.G. Soil erosion prediction using Morgan-Morgan-Finney model in a GIS environment in northern Ethiopia catchment. *Appl. Environ. Soil Sci.* **2014**, *2014*, 468751. [[CrossRef](#)]
40. Shrestha, D.P.; Jetten, V.G. Modelling erosion on a daily basis, an adaptation of the MMF approach. *Int. J. Appl. Earth Obs. Geoinf.* **2018**, *64*, 117–131. [[CrossRef](#)]
41. Mondal, A.; Khare, D.; Kundu, S. A comparative study of soil erosion modelling by MMF, USLE and RUSLE. *Geocarto Int.* **2018**, *33*, 89–103. [[CrossRef](#)]
42. Das, S.; Deb, P.; Bora, P.K.; Katre, P. Comparison of rusle and mmf soil loss models and evaluation of catchment scale best management practices for a mountainous watershed in india. *Sustainability* **2021**, *13*, 232. [[CrossRef](#)]
43. Shen, Z.Y.; Gong, Y.W.; Li, Y.H.; Hong, Q.; Xu, L.; Liu, R.M. A comparison of WEPP and SWAT for modeling soil erosion of the Zhangjiachong Watershed in the Three Gorges Reservoir Area. *Agric. Water Manag.* **2009**, *96*, 1435–1442. [[CrossRef](#)]
44. Mosbahi, M.; Benabdallah, S.; Boussema, M.R. Assessment of soil erosion risk using SWAT model. *Arab. J. Geosci.* **2013**, *6*, 4011–4019. [[CrossRef](#)]
45. Tibebe, D.; Bewket, W. Surface runoff and soil erosion estimation using the SWAT model in the Keleta Watershed, Ethiopia. *Land Degrad. Dev.* **2011**, *22*, 551–564. [[CrossRef](#)]
46. Napoli, M.; Orlandini, S.; Grifoni, D.; Zanchi, C.A. Modelling soil and nutrient runoff yields from an Italian vineyards using swat. *Trans. ASABE* **2013**, *56*, 1397–1406.
47. Pacetti, T.; Castelli, G.; Schröder, B.; Bresci, E.; Caporali, E. Water Ecosystem Services Footprint of agricultural production in Central Italy. *Sci. Total Environ.* **2021**, *797*, 149095. [[CrossRef](#)] [[PubMed](#)]
48. Castelli, G.; Foderi, C.; Guzman, B.H.; Ossoli, L.; Kempff, Y.; Bresci, E.; Salbitano, F. Planting waterscapes: Green infrastructures, landscape and hydrological modeling for the future of Santa Cruz de la Sierra, Bolivia. *Forests* **2017**, *8*, 437. [[CrossRef](#)]
49. Bagarello, V.; Di Piazza, G.; Ferro, V.; Giordano, G. Predictiong unit plot soil loss in Sicily, south Italy. *Hydrol. Process.* **2008**, *22*, 586–595. [[CrossRef](#)]
50. Bagarello, V.; Ferro, V.; Keesstra, S.; Comino, J.R.; Pulido, M.; Cerdà, A. Testing simple scaling in soil erosion processes at plot scale. *Catena* **2018**, *167*, 171–180. [[CrossRef](#)]
51. Wu, S.; Chen, L.; Wang, N.; Zhang, J.; Wang, S.; Bagarello, V.; Ferro, V. Variable scale effects on hillslope soil erosion during rainfall-runoff processes. *Catena* **2021**, *207*, 105606. [[CrossRef](#)]
52. Angeli, L.; Bottai, L.; Costantini, R.; Ferrari, R.; Innocenti, L.; Märker, M. Carta della suscettibilità all'erosione: Analisi e confronto fra modelli di erosione del suolo. *Atti ASITA* **2009**. Available online: <http://atti.asita.it/Asita2005/Pdf/0223.pdf> (accessed on 29 March 2022).
53. ISPRA. *Stato dell'Ambiente—Annuario dei Dati Ambientali*; Geosfera 13/2009 1-23; ISPRA: Roma, Italy, 2016.
54. Zanchi, C.A. Primi risultati sperimentali sull'influenza di differenti colture nei confronti del ruscellamento superficiale e dell'erosione. In *Annali dell'Istituto Sperimentale per lo Studio e la Difesa del Suolo*; Autorità di Bacino del Fiume Arno: Firenze, Italy, 1983; Volume XIV, pp. 277–289.
55. Zanchi, C.A. Influenza dell'azione battente della pioggia e del ruscellamento nel processo erosivo e variazioni dell'erodibilità del suolo nei diversi periodi stagionali. In *Annali dell'Istituto Sperimentale per lo Studio e la Difesa del Suolo*; Autorità di Bacino del Fiume Arno: Firenze, Italy, 1983; Volume 14, pp. 347–358.
56. Rodolfi, G.; Zanchi, C. Caratteristiche fondamentali e dinamica del paesaggio dell'Appennino Tosco Romagnolo. In *Annali dell'Istituto Sperimentale per lo Studio e la Difesa del Suolo*; Autorità di Bacino del Fiume Arno: Firenze, Italy, 1983; Volume XIV, pp. 289–336.
57. Giambastiani, Y.; Giusti, R.; Cecchi, S.; Palomba, F.; Manetti, F.; Romanelli, S.; Bottai, L. Volume estimation of lakes and reservoirs based on aquatic drone surveys: The case study of Tuscany, Italy. *J. Water Land Dev.* **2020**, *46*, 84–96. [[CrossRef](#)]
58. Schweizer, S.; Pini Prato, E. Gestione e tutela (applicazione direttiva nitrati) delle risorse idriche e valutazione degli approvvigionamenti nel settore agricolo ed elaborazione di cartografia tematica (gis) sulle risorse idriche ad uso irriguo. *ARSIA—Reg. Toscana* **2010**, *1*, 1–41.
59. Fernández, C.; Vega, J.A.; Vieira, D.C.S. Assessing soil erosion after fire and rehabilitation treatments in NW Spain: Performance of rusle and revised Morgan-Morgan-Finney models. *Land Degrad. Dev.* **2010**, *21*, 58–67. [[CrossRef](#)]
60. Giannetti, F.; Pegna, R.; Francini, S.; McRoberts, R.E.; Travaglini, D.; Marchetti, M.; Mugnozza, G.S.; Chirici, G. A new method for automated clearcut disturbance detection in mediterranean coppice forests using landsat time series. *Remote Sens.* **2020**, *12*, 3720. [[CrossRef](#)]

61. Borselli, L.; Cassi, P.; Sanchis, P.S.; Ungaro, F.; Menduni, G.; Brugioni, M.; Sulli, L.; Montini, G. *Studio della Dinamica delle Aree Sorgenti Primarie di Sedimento Nell'area Pilota del Bacino di Bilancino: Progetto (BABI); Relazione Attività di Progetto*; Autorità di Bacino del Fiume Arno: Firenze, Italy, 2007. [[CrossRef](#)]
62. Desmet, P.J.J.; Govers, G. GIS-based simulation of erosion and deposition patterns in an agricultural landscape: A comparison of model results with soil map information. *Catena* **1995**, *25*, 389–401. [[CrossRef](#)]
63. Oliveira, A.H.; da Silva, M.A.; Silva, M.L.N.; Curi, N.; Neto, G.K.; de Freitas, D.A.F. *Development of Topographic Factor Modeling for Application in Soil Erosion Models*; InTech: London, UK, 2013; pp. 111–138.
64. Bazzoffi, P. *Erosione del Suolo e Sviluppo Rurale Sostenibile. Fondamenti e Manualistica per la Valutazione Agroambientale*; Il Sole 24 Ore Edagricole: Milan, Italy, 2007; ISBN 8850652283.
65. Borselli, L.; Cassi, P.; Torri, D. Prolegomena to sediment and flow connectivity in the landscape: A GIS and field numerical assessment. *Catena* **2008**, *75*, 268–277. [[CrossRef](#)]
66. Rajbanshi, J.; Bhattacharya, S. Assessment of soil erosion, sediment yield and basin specific controlling factors using RUSLE-SDR and PLSR approach in Konar river basin, India. *J. Hydrol.* **2020**, *587*, 124935. [[CrossRef](#)]
67. Vanoni, V.A. *Sedimentation Engineering*; American Society of Civil Engineers: New York, NY, USA, 1975; 745p.
68. Ferro, V.; Porto, P. Sediment delivery distributed (sedd) model. *J. Hydrol. Eng.* **2000**, *5*, 411–422. [[CrossRef](#)]
69. Saygin, S.D.; Ozcan, A.U.; Basaran, M.; Timur, O.B.; Dolarslan, M.; Yilman, F.E.; Erpul, G. The combined RUSLE/SDR approach integrated with GIS and geostatistics to estimate annual sediment flux rates in the semi-arid catchment, Turkey. *Environ. Earth Sci.* **2014**, *71*, 1605–1618. [[CrossRef](#)]
70. Li, P.; Mu, X.; Holden, J.; Wu, Y.; Irvine, B.; Wang, F.; Gao, P.; Zhao, G.; Sun, W. Comparison of soil erosion models used to study the Chinese Loess Plateau. *Earth-Sci. Rev.* **2017**, *170*, 17–30. [[CrossRef](#)]
71. Angeli, L.; Costantini, R.; Costanza, L.; Ferrari, R.; Gardin, L.; Innocenti, L. *Rapporto Finale Ufficiale Sulla Realizzazione Della "Carta del Rischio di Erosione Idrica Attuale Della Regione Toscana in Scala 1:250.000"—Region Toscana*; Consorzio LaMMA: Sesto Fiorentino, Italy, 2004.
72. Tauro, F.; Petroselli, A.; Fiori, A.; Romano, N.; Rulli, M.C.; Porfiri, M.; Palladino, M.; Grimaldi, S. "Cape Fear"—A hybrid hillslope plot for monitoring hydrological processes. *Hydrology* **2017**, *4*, 35. [[CrossRef](#)]
73. Tazioli, A. Evaluation of erosion in equipped basins: Preliminary results of a comparison between the Gavrilovic model and direct measurements of sediment transport. *Environ. Geol.* **2009**, *56*, 825–831. [[CrossRef](#)]
74. Romano, N.; Nasta, P.; Bogena, H.; De Vita, P.; Stellato, L.; Vereecken, H. Monitoring Hydrological Processes for Land and Water Resources Management in a Mediterranean Ecosystem: The Alento River Catchment Observatory. *Vadose Zone J.* **2018**, *17*, 180042. [[CrossRef](#)]